Silver Electrocrystallization onto Carbon Electrodes with Different Surface Morphology: Active Sites vs Surface Features

ARTICLE *in* THE JOURNAL OF PHYSICAL CHEMISTRY B · APRIL 2001

Impact Factor: 3.3 · DOI: 10.1021/jp002057d

3 AUTHORS, INCLUDING:

Margarita Miranda-Hernández
Universidad Nacional Autónoma de México
28 PUBLICATIONS **406** CITATIONS
SEE PROFILE

Ignacio Gonzalez
Metropolitan Autonomous University
280 PUBLICATIONS **3,492** CITATIONS
SEE PROFILE

Silver Electrocrystallization onto Carbon Electrodes with Different Surface Morphology: Active Sites vs Surface Features

M. Miranda-Hernández,[†,‡] I. González,[†] and N. Batina*[,†]

Universidad Autónoma Metropolitana-Iztapalapa, Dpto Química, Área de Electroquímica, A.P. 55-534, 09340 México. D.F. (México), and Instituto Mexicano del Petróleo, Coordinación de Simulación Molecular, Área de Materiales y Corrosión, Eje Central Lázaro Cardenas No. 152, C.P. 07730, México, D.F. (México)

Received: June 7, 2000; In Final Form: November 5, 2000

The influence of the electrode surface quality and surface morphology on the silver electrocrystallization process onto a carbon substrate from 10^{-2} M $Ag(NH_3)_2^+$/1.6 M NH_3, 1 M KNO_3 (pH = 11) electrolyte solution was studied. Three substrates with different types of surface morphology and surface roughness were used: highly oriented pyrolitic graphite (HOPG), mechanically polished vitreous carbon (MPVC), and fractured vitreous carbon (FVC). Before the silver deposition process, the electrode surface was examined and characterized by means of Atomic Force Microscopy (AFM) analysis. Evaluation of the kinetic parameters of the silver nucleation and the growth behavior, as well as other characteristics of the silver electrocrystallization process onto carbon substrates, were based on cyclic voltammetry and chronoamperometric measurements. Cyclic voltammetry data also show that silver deposition efficiency is proportional to the increase of electrode surface roughness (from HOPG, via MPVC to FVC). The silver bulk deposition process on all three carbon substrates was characterized as 3D nucleation and diffusion-controlled growth. However, this process proceeds with different overpotentials on different substrates: the lowest for HOPG and the highest for MPVC electrode surface. The major electrocrystallization parameters, such as nucleation rate, number of active sites, and number of formed silver nuclei, strictly related to the electrode surface conditions, seem to not follow the same trends as the cyclic voltammetry data. It is clearly indicated in the nonlinear relationship between number of active sites and the surface features (recognized in AFM images). As pointed out in the discussion, it opens new questions regarding the nature of the active sites for deposition on the electrode surface and their identification by microscopic techniques.

1. Introduction

In modern electroanalytical chemistry, particularly for technological use, carbon is the most common electrode material. It comes in many different forms: amorphous (glassy or "vitreous"-VC- carbon), crystalline-pyrolitic graphite (i.e., HOPG), reticulated vitreous carbon (RVC), and so forth. Although in all cases the building material is the same, carbon, it differs in surface structure and surface properties, which influence and control its electrochemical and chemical activity.[1−3]

So far, many studies have been devoted to the influence of the different surface preparations (chemical and electrochemical pretreatment) of carbon electrodes in order to understand and alter their properties. Typically, such carbon electrode pretreatment processes lead to electrode surface "activation", which speeds up the redox process (i.e., hexacyanoferrate (III)−(II),[3−11] or even increases the amount of molecular adsorbate at the electrode surface.[3−6,9,10,12−14] Because the "activation" is related, in many aspects, to the electrode surface conditions, it triggers interest in the detailed characterization of the electrode surface (surface morphology, surface roughness, and fractal characteristics), by scanning electron microscopy (SEM) or, more recently, from the scanning probe microscopy SPM techniques.[3,5,15−24] Most results point out the surface cleanness influence, rather than the surface roughness, as the dominant parameter for electrode activity control. However, it has been clearly demonstrated that differently pretreated electrodes possess different morphologies of their top surface layer and that this has an influence on the surface reaction process. As a very important fact, one should note that the relationship between electrochemical activity and surface conditions (i.e., surface quality, from a macroscopic point of view), so far, has been established only for a few selected surface reactions (redox process of nonadsorbed species, molecular adsorption).

As we know, Bodalbhai and Brajter-Toth[22] were the first to try to establish a relationship between the electrode surface topography and the copper deposition process using differently pretreated graphite electrodes. From our point of view, it is a very interesting case because the metal deposition process is an electrocrystallization phenomenon that progresses exclusively via selective areas, so-called "active sites" and does not involve the whole surface (macroscopically) like the molecular adsorption process, for example.[25] They concluded that microscopic surface roughness is not a source of electrode activity. In other words, the increase in the surface roughness is not the exclusive cause of the surface activity increase for pretreated graphite surfaces.

The aim of our work is to investigate the influence of the electrode surface conditions (surface morphology and surface

* To whom correspondence should be addressed. Tel: (52) 5804-4671. Fax: (52) 5804-4666. E-mail: bani@xanum.uam.mx.

[†] Universidad Autónoma Metropolitana-Iztapalapa, Dpto. Química, Área de Electroquímica.

[‡] Instituto Mexicano del Petróleo, Coordinación de Simulación Molecular, Área de Materiales y Corrosión.

10.1021/jp002057d CCC: $20.00
Published on Web 04/13/2001

roughness) on the silver electrocrystallization process. Combining the power of AFM and the interpretation of current-transient data, we attempt to understand the relation between the deposition active sites, the silver nuclei, and the electrode surface morphology. One of our greatest concerns was the relationship between surface features and the deposition nuclei, which also triggers a new question about the possibility of visualization and identification of the active sites and early metallic nuclei on the electrode surface by SPM techniques.

This work is a part of our long-time effort to investigate the details of the metal deposition mechanism and their visualization by SPM techniques. See our recently published papers about the influence of roughness and fractality of the electrode surface on the efficiency of the lead deposition onto differently pretreated vitreous carbon, refs 26 and 27, or the influence of the concentration of active species on the deposition mechanism, refs 28 and 29.

2. Experimental Section

The electrochemical techniques, cyclic voltammetry, and chronoamperometry were employed to study silver electrocrystallization onto a carbon substrate. All of the electrochemical experiments were carried out in a conventional three electrode cell system with a working carbon electrode, a reference electrode (saturated calomel electrode, SCE), and a counter electrode (a graphite road with large surface area). Three different types of carbon electrodes, prepared from vitreous carbon (VC) and highly oriented pyrolitic graphite (HOPG) material, were used in our study. The HOPG-electrodes were prepared from graphite provided by Union Carbide Corp., USA. Before each experiment, HOPG-electrodes were cleaved with adhesive tape to peel the top adlayers and prepare a new "defect-free" surface. VC-electrodes were prepared from a carbon rod (Johnson Mattey & AESAR, 5 mm diameter) and used either as fractured vitreous carbon (FVC) or as mechanically polished vitreous carbon (MPVC) electrodes. The FVC electrodes were prepared by the manual fracturing of the carbon rod, just before each experiment. The sides of the FVC electrode were isolated by a PTFE film, such that only the fractured portion of the electrode surface came into contact with the electrolyte solution. PMVC-electrodes were prepared by being polished with 600-grit silicon carbide paper followed by 1− and 0.3 μm alumina/water suspension on polishing cloth (Buehler, USA). After polishing, the PMVC-electrodes were rinsed with pure water and treated in an ultrasonic bath for 5 min.

The electrode potential in electrochemical experiments was controlled by a PAR 273 potentiostat coupled with a computer. The silver deposition was carried out from electrolyte solution containing: 10^{-2} M $AgNO_3$, 1.6 M NH_3 and 1 M KNO_3, at pH = 11. As demonstrated before, under these particular conditions Ag(I) is predominantly present in an $Ag(NH_3)_2^+$ complex form.[28−30]

Cyclic voltammetry was performed in the potential range between 0.70 V and −0.70 V versus SCE, with a scan rate of 50 mV/s. Chronoamperometric experiments were performed by using a cathodic pulse between 0.10 and −0.70 V versus SCE. At the resting potential (0.70 V vs SCE), the electrode was free of silver deposit. All of the solutions were prepared using reagent grade chemicals and ultrapure Milli-Q water.

Prior to the silver deposition, the surface of the carbon electrodes: HOPG, FVC and MPVC was characterized by Atomic Force Microscopy (AFM). A Nanoscope III-multimode AFM from Digital Instruments, USA, was operating in the contact mode under laboratory conditions (ex-situ). Si_3N_4 tips, with standard geometry mounted on the gold cantilevers, were used to acquire the topographical images. Imaging was performed with a rather slow scan rate of 1 Hz, to avoid possible sample damage. All of the images in the paper are presented in the so-called "height mode", where the higher parts appear brighter, and as a 3D graphic. Morphological characteristics of the carbon electrode surface, such as surface roughness, were quantitatively evaluated using the software package for image analysis, which accompanies the Nanoscope III system.

3. Results and Discussion

3.1 Electrode Surface Characterization. The surface morphology of HOPG-, MPVC-, and FVC-electrodes, prior to the silver deposition process, was examined by Atomic Force Microscopy (AFM). The main goal was to determinate and characterize a possible difference among the surface morphologies of the carbon electrodes used here, which could influence the course of the silver deposition process. A set of typical AFM images obtained for carbon surfaces tested in our study, acquired under identical imaging conditions, is shown in Figure 1. The images clearly revealed that the electrodes used differ in surface morphology. The surface of the HOPG-electrode appears to be smooth with large (up to several μm wide), atomically flat terraces, occasionally separated by atomic steps (Figure 1a.). In short, this is a typical morphology of the monocrystalline materials. To describe the electrode surface more quantitatively, and to provide a quantitative comparison of the surface quality among the tested electrodes, we employed the root−mean−square roughness RMS[Rq] function. Although, as well pointed out in one of the previously published papers,[24] RMS[Rq] has not been established as a rigorous quantitative measure of the surface roughness and the surface quality, it has often been used for such purpose. Apparently, it is one of the simplest morphology parameters that can be used for the surface quality description.[24,27,31−34] For HOPG-electrodes, we found that the average [RMS]Rq is 0.58 ± 0.07 nm, which is also sufficiently close to the previously reported value.[24]

Contrary to the smooth and somehow homogeneous (in terms of morphology) surface of the HOPG-electrodes, the AFM image in Figure 1b revealed a large number of rather small features randomly distributed all over the FVC-electrode surface. The FVC surface was described more quantitatively in one of our previous papers.[27] Therefore, we would like to mention that the nodular surface features are of rectangular or ellipsoidal shape with the following dimensions: 120−150 nm by 65 nm. Such an FVC-texture appears to be very similar to one previously observed in STM studies.[23,24] The RMS[Rq], estimated in our experiments (8.5 ± 0.5 nm) is significantly lower than that of the value reported in a previous study (20 ± 0.5 nm).[24] We believe that this is due to difference in the image acquiring mechanism between the STM and the AFM techniques.

A typical morphology of the MPVC-electrode surface is shown in Figure 1c. Similar to the FVC surface texture, the AFM images of the MPVC-electrode surface revealed mainly nodular features. However, they appear to be of different shape and lower height than those observed at the FVC surface. As expected, the MPVC-electrode surface possessed a lower RMS-[Rq] value (3.5 ± 0.5 nm) than that of the FVC-electrode surface. This is in a good agreement with the previously reported value of 4.1 ± 1 nm.[24] In comparison with other electrodes, it is obvious that the HOPG surface is the smoothest and that the surface roughness of FVC decreases during polishing.

3.2 Voltammetric Study. To evaluate the influence of the electrode morphology on the metal electrocrystallization process,

all three electrodes (FVC, MPVC, and HOPG) were subjected to the same kind of silver deposition process. This was carried out from a solution containing 10^{-2} M Ag(I) as $AgNO_3$ salt, 1.6 M NH_3, and 1 M KNO_3 with pH adjusted to 11. As demonstrated before, under these conditions, the electroactive species, Ag(I), predominately has a form of the $Ag(NH_3)_2^+$ complex.[28−30] The silver deposition process follows the reaction described by eq 1, at the equilibrium potential described by eq 2[28−30]

$$Ag(NH_3)_2^+ + e^- \rightleftarrows Ag^\circ + 2NH_3 \quad (1)$$

$$E = E^\circ_{Ag(NH_3)_2^+} + 0.06 \log \frac{[Ag(NH_3)_2^+]}{[(NH_3)]^2} \quad (2)$$

For our experimental conditions, E was estimated to be −0.008 V vs SCE.

Figure 2 shows a set of voltammograms obtained for silver deposition/dissolution on three carbon electrodes: FVC, HOPG, and MPVC, which, according to AFM analysis, possess different surface morphology. In each experiment, the voltammetric scan starts from 0.700 V versus SCE toward the negative potentials (−0.700 V vs SCE) with scan rate of 50 mV/s. As is apparent, all three of the voltammograms possess similar shape, with one characteristic peak obtained during the cathodic scan and a second obtained during the anodic scan. According to the previous description, the cathodic peak is related to the silver deposition process (formation of silver deposit on the carbon electrode), whereas the anodic one is related to the silver dissolution process.[28−30] Regardless of the type of the carbon substrate, the silver deposition and the dissolution peaks always appear at the same potential (see values for Epc and Epa in Table 1), which indicates the same type of process (energetic and kinetic sense) on all three electrodes. However, the height of voltammetric peaks and the amount of charge estimated from the surface area under peaks, for scans in both directions (Qpc and Qpa), indicate significant differences. Presumably, they indicate that the amount of charge is a measure of the deposited or dissolved silver (depending on the scan direction), so it is clear that silver deposition efficiency changes depending on the type of carbon electrode. Thus, a decrease in efficiency was found for PMVC and, in particular, for the HOPG electrode during the deposition and dissolution process (Table 1). Note that in all experiments, the silver deposition was carried out under the same conditions, from the same electrolyte solution with the same concentration of the electroactive species and within the same potential range. Although HOPG, FVC, and MPVC differ, from structural point of view, and the electronic properties indicate that they are possibly not exactly the same substrates, the easiest way to explain the observed differences in the silver deposition efficiency is the dependence of the current on the electrode area. As it is well established, the current response in the cyclic voltammogram is directly proportional to the electrode area,[35] which commonly means the electrode area is defined as two-dimensional geometric surface. However, there are also plenty of examples where specific area, or "total active surface area", was used instead. In this case, the electrode surface was defined as a three-dimensional object, with significant surface roughness.[17,21,24,36−38] For example, it was demonstrated that the amount of adsorbed material on the electrode surface depends on the electrode conditions (surface roughness).

The first consideration of the data in Table 1 shows the same trend. The highest level of deposit was achieved on FVC, the

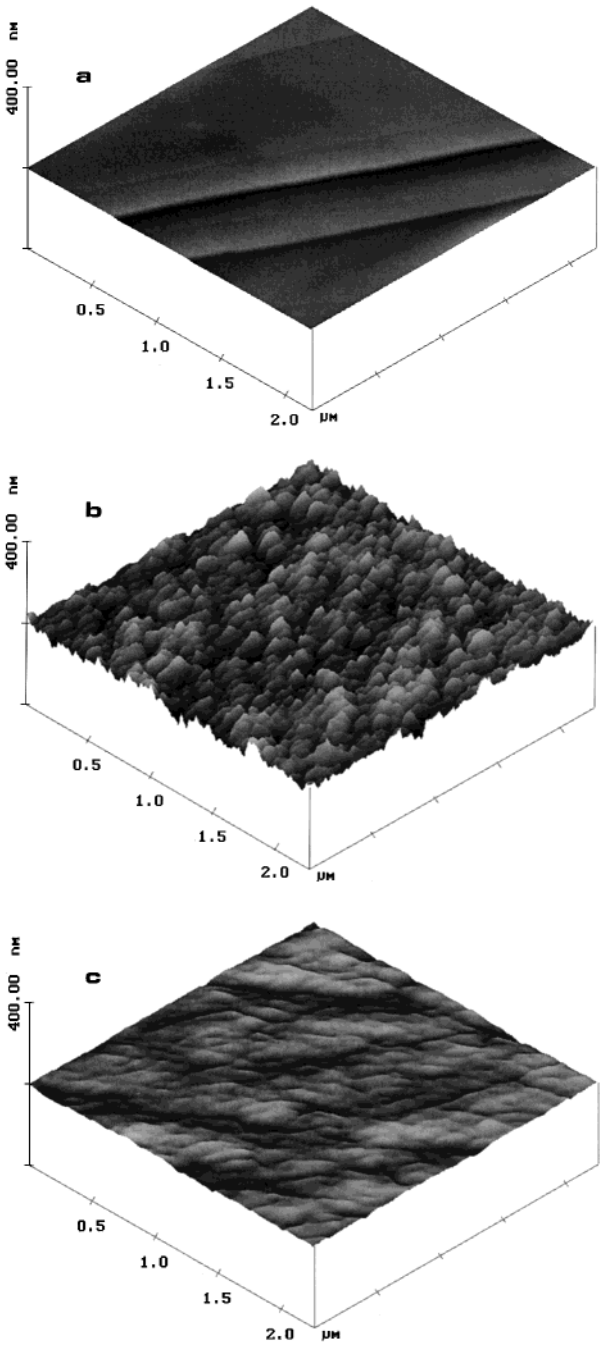

Figure 1. AFM images (2.20 μm × 2.20 μm) show the characteristic surface morphology for different carbon electrode substrates: (a) Highly oriented pyrolitic graphite (HOPG), (b) Fractured vitreous carbon (FVC) and (c) Mechanically polished vitreous carbon (MPVC).

electrode with the highest roughness (the higher RMS [Rq] factor, see AFM section above). The very flat HOPG appears to have a 50% decrease in the silver deposit amount compared to FVC. To establish a more precise relationship between the silver deposition efficiency and the electrode surface morphology properties, we plotted the RMS [Rq] versus charge amount (Qpc) consumed during the silver deposition process for all three electrodes used in our experiments (Figure 3). The plot indicates linear relation between RMS [Rq] versus Qpc, which means that the higher amount of deposit is expected on the electrode with the higher roughness. However, to increase the amount of the deposited silver two-times, the RMS [Rq] factor should increase almost eighteen times, which leads to a proportionality coefficient different than one. Another interesting thing is the

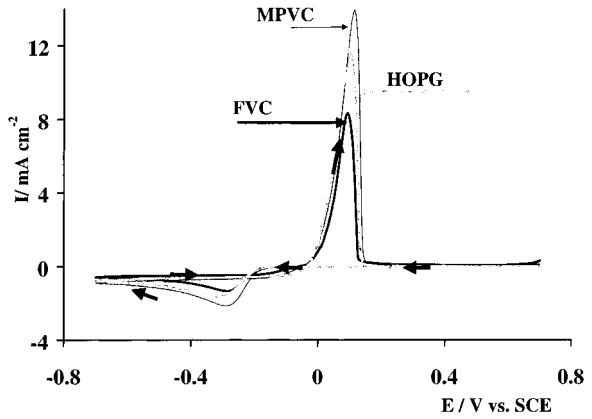

Figure 2. Cyclic voltammograms for the $Ag(NH_3)_2^+$ deposition process obtained onto HOPG, FVC, and MPVC electrodes, from 10^{-2} M $Ag(NH_3)_2^+$/1.6 M NH_3, 1 M KNO_3 electrolyte solution. Scan rate: 50 mV/s.

relationship of those data with the total active surface area. Namely, one can see from Table 1, that the Qpc for FVC and MPVC differs by a factor 1.57, which is nearly close to the fact that the FVC surface was found to have a microscopic area 1.8 times that of the polished surface.[23] Therefore, it seems that the increase in Qpc for FVC can be attributed to the increase of the active surface area. However, looking again into Table 1, one could also see that the surface roughness (RMS[Rq]) of the FVC electrode is 2.83 times higher than that for MPVC, which tells us that the changes in the silver deposition efficiency cannot be attributed only to the variation in the electrode surface roughness. Some previous studies also report the absence of a direct correlation between the electrochemical response on carbon electrodes and the surface roughness.[13,22] The last report is particularly important for our study because the deposition of metal species onto a carbon electrode and its relation to the surface roughening was studied. In addition, the results of many studies indicate that the kinetics and the electrochemical activity of the carbon electrode surface depends on the nature of the electrochemical reaction (see ref 3 and the references cited therein]. Because metal deposition is an electrocrystallization process that is mainly associated with the formation of early nuclei around the active sites on the electrode surface, we expected that besides the macroscopic parameter, such as the total active surface area, deposition onto a substrate with a different morphology will also lead to a different mechanism, due to a different distribution, density, size, and other characteristics of the deposition active sites. Note that in the case of ionic or molecular adsorption, often studied in relation to the substrate characteristics, the determination of the total active surface area could be sufficient.[17] The metal deposition process, which specifically acts via active sites, is far more complex, in particular because the nature of the "active sites" is often unclear.

3.3 Chronoamperometric Study. Chronoamperometric studies were performed to investigate the influence of the carbon electrode surface morphology onto the mechanism of the silver deposition process. As one could suppose, our interest was to determine the relation between the silver deposition active sites and different surface morphology of the carbon electrodes. In particular, we would like to see whether the increase in the electrode surface roughness, which, according to the cyclic voltammetry, leads to the increase in deposited silver, was the result of the increase in deposition active sites.

Chronoamperometric measurements based on the current-transients recording are an excellent choice for such study because using the appropriate models offers information about active sites, electrocrystallization kinetics, and other details of the nucleation process, usually not available with other techniques. The method and approach that we are using here has been described in our previous papers.[28,29] Like in the voltammetric study, the silver deposition was carried out from ammoniacal bath containing 10^{-2} M $Ag(NH_3)_2^+$ in 1.6 M NH_3 and 1.0 M KNO_3 pH = 11. Current-transients were recorded after steeping the electrode potential from the positive potential limit (0.70 V vs SCE), where silver adsorption does not take place, to the potential region more negative than −0.008 V versus SCE, in which silver deposition occurs. The negative potential limit was different; it depended on the substrate and varied from −0.15 V to −0.38 V versus SCE. To compare charge consumption during the deposition process, 20 s potential steps were always used. To avoid memory effect, after each recording, the electrode surface was renewed by additional mechanical polishing (MPVC) or just simply replaced with a new electrode (FVC, HOPG).

The current transients obtained for HOPG, MPVC, and FVC electrodes are shown in Figure 4. Although all transients were recorded during 20 s, they are presented with a different time scale, to emphasize the transient shape. As it could be seen, all transients are of the same shape, with characteristic and well-defined current maxima. At higher overpotentials, transient maxima are more defined but shifted toward shorter times. According to these characteristic shapes, every current transient presented in Figure 4 can be associated with the same model, quantitatively described by Scharifker et al.[25,38−41] and based on a 3D nucleation process controlled by diffusion of the electroactive species. Careful comparison reveals that the transients were obtained at different electrode potentials, which indicates that the application of different overpotentials was necessary to start the silver 3D-electrocrystallization process. On a HOPG substrate, the 3D silver deposition started already at −0.050 V versus SCE; thus, for FVC and MPVC, it was necessary to reach the more negative potentials (higher overpotential) of −0.150 V and −0.300 V versus SCE, respectively. We believe that the reason for the higher overpotential is most likely to be found among the energetic conditions on the electrode surface, including density and characteristics of the active sites for the deposition process. Interestingly, the cyclic voltammetry shows that all surfaces possess deposition peaks at very similar potentials, which indicates that the peak in the voltammogram is not necessarily related only to the silver 3D deposition process. Also, as is well-known, voltammetric peaks are very much affected by kinetics of the electrochemical process and, therefore, are not very suitable and recommended for the evaluation of the electrocrystallization parameters.[42]

The diffusion coefficient, D, for the $Ag(NH_3)_2^+$ species on each substrate was estimated using the Cottrell equation, eq 3, and analyzing the behavior of current transients in the part just after the maximum (declining current region). The Cottrell equation is described as

$$i(t) = \frac{\mathrm{nF}AD^{1/2}\mathrm{C}}{\pi^{1/2}t^{1/2}} \qquad (3)$$

where nF is the molar charge transferred, C is the bulk concentration of silver species, A is the geometric area of the electrode, and D is the diffusion coefficient.

It is important to note that the D values were estimated considering the geometric area of surface electrode. Although the difference between those substrates was not large, the trend among the values was interesting. The HOPG current transients

TABLE 1: Values of Potential (*E*p) and Charge (*Q*p) for Cathodic-Deposition (*c*) and Anodic-Dissolution (*a*) Peaks Estimated from Voltammograms Presented in Figure 2, for Silver Deposition Process onto Different Carbon Electrode Substrates, with Corresponding RMS[Rq] Values, as a Measure of the Electrode Surface Roughness[a]

electrode	*Epc*/*V* vs. SCE	*Epa*/*V* vs. SCE	*Q*pc/mC cm^{-2}	*Qpa*/mC cm^{-2}	RMS [Rq]/nm
HOPG	−0.315	0.098	−18.75	18.07	0.58 ± 0.07
MPVC	−0.288	0.103	−22.30	21.40	3.0 ± 0.50
FVC	−0.286	0.096	−35.06	31.50	8.5 ± 0.50

[a] Evaluation of the surface roughness factor was based on an AFM image analysis.

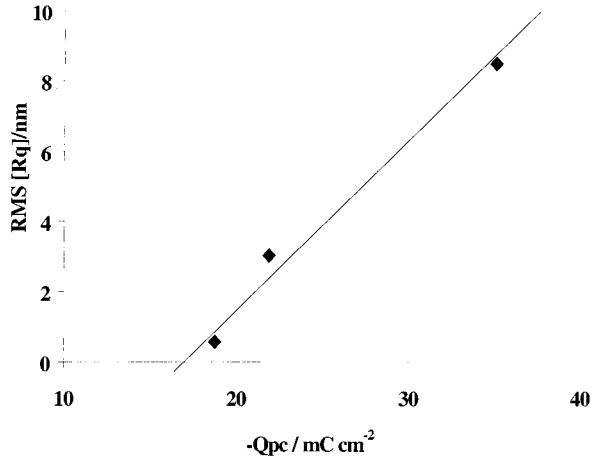

Figure 3. Relationship between the electrode surface roughness factor (RMS[Rq]) and the total amount of charge evaluated under the cathodic peak (Qpc) during a silver deposition process onto different carbon electrodes. The RMS[Rq] factor was evaluated from AFM images (Figure 1).

show two times higher *D* than those obtained for FVC and MPVC substrates. The *D* value for MPVC was found to be around 1.0 × 10^{-5} cm^{-2}s^{-1}, which is very close to the previously published value for the mechanically polished electrodes.[28,43] FVC has an average *D* around 1.4 × 10^{-5} cm^{-2}s^{-1}, and HOPG around 3.5 × 10^{-5} cm^{-2}s^{-1}. Those *D* values follow the inverse order, as the overpotential required the start of the 3D silver deposition process. The HOPG surface needs less overpotential for starting and acting with a faster rate. Note that in an energetic sense, the silver deposition onto MPVC has difficulties because a rather large overpotential is necessary to start the 3D process. Also, it is worth noticing that the HOPG substrate with the higher *D* value is also the smoothest surface (RMS [Rq] = 0.58 ± 0.05 nm). MPVC and FVC, with higher surface roughness, possess lower *D* coefficients. The diffusion process of Ag $(NH_3)_2^+$ to the surface electrode may be dependent on the electrode surface condition. The difference of *D* values, obtained considering the geometric area, show the influence of the "real area" into the D evaluation. These results suggest that the "real area" depends on the surface roughness and the potential conditions of the surface, but unfortunately, we cannot show the relationship between those parameters.

The theoretical model of Scharifker et al.[25,38−41] for the 3D diffusion-controlled nucleation and growth process, was used for the further analysis. As a preliminary step, all current transients were presented in a nondimensional form, normalized current versus time [$(I/I_m)^2$ vs t/t_m] plot. I_m and t_m correspond to the maximum current and time values used in the normalization processes. According to this methodology, often used in previous studies,[28−30,44,45] a comparison of the theoretical plots with the experimental data allows the determination of nucleation process mechanism: instantaneous versus progressive. Figure 5 shows such nondimensional plots for silver deposition on HOPG, MPVC, and FVC substrates. As it can be seen very clearly, the relationship between the experimental curves and the theoretical models are the same in all three cases, regardless of the substrate. In general, the nucleation mechanism changes in dependence on the applied potential (overpotential). At lower overpotentials, nucleation appears to be progressive, but at higher overpotentials it changes toward the instantaneous kind. As we demonstrated in some of our previous papers,[29,30] in the case when the nucleation mechanism changes with the applied overpotential, the evaluation of kinetic parameters based on the nondimensional [$(I/I_m)^2$ vs t/t_m] plots, cannot be used.

Therefore, to estimate the kinetic parameters for silver 3D-deposition, we used Scharifker's[30,44,45] general equation, eq 4, for the time evolution of the current density via a 3D nucleation process limited by diffusion control growth as an alternative method. This equation is equally valid for describing instantaneous and progressive nucleation and does not require the classification of the nucleation mechanism, prior to its use

$$I(t) = \left(\frac{zFD^{1/2}C}{\pi^{1/2}t^{1/2}}\right)\left(1 - \exp\left\{-N_0\pi kD\left[t - \frac{1 - \exp(-At)}{A}\right]\right\}\right) \quad (4)$$

Where the number density of active sites is N_0, the nucleation rate constant is *A*, other parameters are as defined above, and eq 5 defines *k*

$$k = \frac{4}{3}\left(\frac{8\pi CM}{\rho}\right)^{1/2} \quad (5)$$

where *M* and ρ are the atomic weight and the density of the deposited material, respectively. The saturation number density of the formed silver nuclei *N*s, was calculated by using eq 6[30,40]

$$Ns = \sqrt{(AN_0/2kD)} \quad (6)$$

The experimental data program were adjusted by a nonlinear fitting of eq 4, using the EQ001 program proposed by Mostany and Scharifker.[44−46]

Table 2 shows the kinetic parameters for silver electrocrystallization process: the nucleation rate *A*, the number density of active sites N_0, and the saturation number density of the formed silver nuclei *N*s. They were evaluated from our experimental current transients for HOPG, MPVC, and FVC electrode substrate, using the above-described equations. Table 2, also shows values for the *N*s/N_0 ratio and the total charge density recorded during the applied potential step. Charge densities were calculated from the area under current-transients.

During analysis and interpretation of the data from Table 2, we established the general trends and dependence of the deposition kinetic parameters on the electrode potential. In the next step, priority was a comparison between the kinetic parameters of the silver electrocrystallization onto HOPG, MPVC, and FVC substrates and their relation to the morphological properties (surface roughness) of the used electrodes.

As it was expected in accordance with the theory and previous findings,[46,47] we found that: *Q*, *A*, N_0, and *N*s increase with the

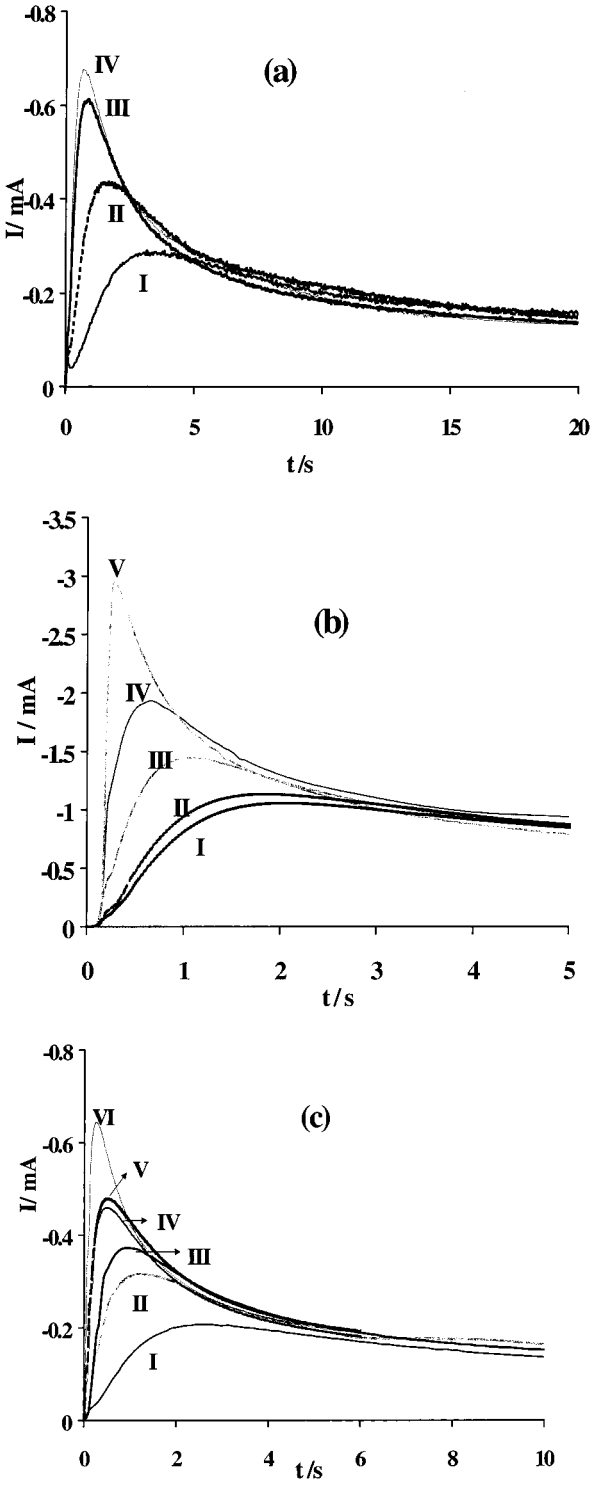

Figure 4. Set of experimental current transients obtained in 10^{-2} M $Ag(NH_3)_2^+$/1.6 M de NH_3, 1 M KNO_3, and pH = 11 for silver deposition process onto different carbon electrode substrates: (a) HOPG, (b) MPVC, and (c) FVC. The imposed potentials at electrode were: (a) HOPG: (I) −0.05 V; (II) −0.10 V; (III) −0.12 V; and (IV) −0.15 V vs SCE. (b) MPVC: (I) −0.30 V; (II) −0.32 V;(III) −0.35 V; (IV) −0.36 V; and (V) −0.38 V vs SCE. (c) FVC: (I) −0.15 V; (II) −0.22 V;(III) −0.24 V; (IV) −0.26 V;(V) −0.28 V; and (VI) −0.030 V vs SCE All potential steps were initiated at 0.70 V vs SCE.

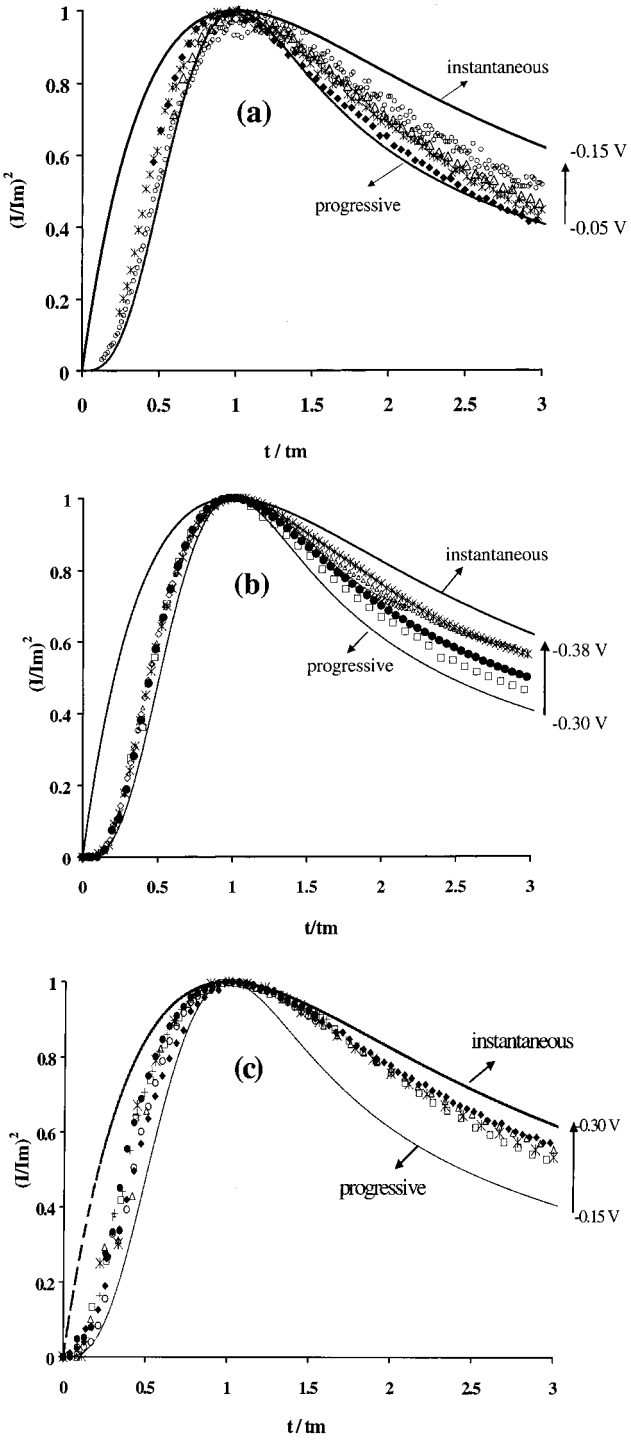

Figure 5. Comparison between experimental (points) and theoretical (lines) current transients obtained for silver deposition onto: (a) HOPG, (b) MPVC, and (c) FVC presented in the nondimensional $(I/I_m)^2$ vs t/t_m plot. Theoretical transients for instantaneous and progressive nucleation (limited case), were calculated according to the Scharifker model.[44] Deposition was carried out from 10^{-2} M $Ag(NH_3)_2^+$/1.6 M de NH_3, 1 M KNO_3 (pH = 11) solution at the imposed potentials, within a range marked on each figure: HOPG: (△) −0.05 V; (*) −0.10 V; (○) −0.12 V; and (◆) −0.15 V. MPVC: (△) −0.30 V; (◆) −0.32 V; (*) −0.35 V; (●) −0.36 V; and (◇) −0.38 V. FVC: (△) −0.15 V; (○) −0.20 V; (*) −0.22 V; (□) −0.24 V; (●) −0.26 V; (+) −0.28; and (◆) −0.30 V.

application of the negative electrode potential. Indeed, the same kind of behavior was found for all three electrode substrates, which is, as we believe, related to the fact that the deposition process is driven by the electrode potential (deposition overpotential). Usually, the higher overpotential is associated with higher efficiency, Q and N_0, as found in our study, as well. The Ns/N_0 ratio, which can also be defined as the efficiency of use of the surface available nucleation sites, decreases at more negative electrode potentials. At least this trend is clear for the

TABLE 2: Potential Dependence of the Kinetic Parameters Describing Silver Nucleation on Different Carbon Substrates: (*A*) Nucleation Rate, (N_0) Number Denisty of Active Sites, (*N*s) Number Density of the Formed Silver Nuclei, Total Amount of the Charge (*Q*)[a]

		HOPG			RMS[Rq] = 0.58 ± 0.05 nm
E/*V* vs. SCE	*A*/*s*	$N_0 \times 10^{-6}$/cm^{-2}	*N*s $\times 10^{-6}$/cm^{-2}	*N*s/N_0	*Q*/mC cm^{-2}
−0.05	1.06	5.70	2.54	0.45	−11.61
−0.10	0.29	6.10	0.94	0.15	−14.98
−0.12	0.08	25.50	1.03	0.04	−15.66
−0.15	0.17	21.70	1.35	0.06	−16.72
		MPVC			RMS[Rq] = 3.0 ± 0.5 nm
E/*V* vs. SCE	*A*/*s*	$N_0 \times 10^{-6}$/cm^{-2}	*N*s $\times 10^{-6}$/cm^{-2}	*N*s/N_0	*Q*/mC cm^{-2}
−0.30	0.95	0.51	0.35	0.68	−8.49
−0.32	1.33	0.69	0.35	0.50	−8.72
−0.34	2.22	0.75	0.47	0.63	−9.88
−0.35	2.48	0.92	0.55	0.60	−9.49
−0.36	2.57	1.07	0.60	0.56	−10.01
−0.38	3.01	1.53	0.78	0.50	−9.42
		FVC			RMS[Rq] = 8.5 ± 0.5 nm
E/*V* vs. SCE	*A*/*s*	$N_0 \times 10^{-6}$/cm^{-2}	*N*s $\times 10^{-6}$/cm^{-2}	*N*s/N_0	*Q*/mC cm^{-2}
−0.15	0.35	1.40	0.62	0.46	−8.3
−0.20	0.14	14.07	1.28	0.09	−10.8
−0.22	0.31	13.23	1.82	0.14	−11.4
−0.24	1.07	9.70	2.90	0.29	−10.5
−0.26	0.92	11.40	3.02	0.25	−11.0
−0.28	2.52	5.00	3.24	0.64	−11.7
−0.30	6.73	8.20	6.75	0.82	−12.6

[a] Obtained for silver electrocrystallization from 10−2 M $Ag(NH_3)_2^+$/1.6 M de NH_3, 1 M KNO_3 (pH = 11).

HOPG electrode. For MPVC, the *N*s/N_0 ratio is rather constant, and in the case of FVC, it was not easy to define the course of changes.

As a second step of our analysis, we tried to compare kinetic parameters of different substrates, hoping to find a general dependence of the deposition kinetic on the substrate characteristics. Results of our analysis appeared to be very complex and unexpected. For example, the charge density *Q* and number density of active sites N_0 reached the highest values for the HOPG substrate. A decrease in *Q* and N_0 was determined for FVC and MPVC substrates, respectively. If simply assuming that higher consumption of charge is related to the larger amount of the silver deposit, it means that the amount of deposit (efficiency of deposition) decreases in the following order: HOPG, FVC, and MPVC. Furthermore, the same trend for *Q* and N_0 can be interpreted in the fashion of more active sites−more deposit. Thus, we suppose that MPVC is the least among those tested because mechanical polishing induces an oxide layer on the carbon electrode surface,[24] which probably blocks some of the available active sites for the silver deposition process.

However, the remaining question is why HOPG possesses much more active sites for the silver deposition than those of FVC and MPVC. According to previous studies, mostly based on evaluation of the heterogeneous electron-transfer rate constant for redox systems in solution ($Fe(CN)_6^{3-/4-}$ and dopamine) the chemical and electro-chemical activity of carbon electrodes depend on the number of surface defects.[3,8924] The edge plane HOPG has more active sites for electron transfer and shows higher electron-transfer rate than basal that of HOPG. The same trend has been seen after comparing FVC and HOPG,[3] where FVC presents more rugosity and much more reactivity. Bodalbhai and Brajter-Toth[22] studied the copper electrodeposition onto graphite electrodes and found that increase of the copper active sites can be correlated to the increase in the electrode roughness and electron-transfer kinetics for $Fe(CN)_6^{3-/4-}$. They concluded that the same treatment that increases the density of cooper nucleation sites also increases the electron-transfer rate.

From our data (see Table 2), it is clear that HOPG is the substrate with the most available active sites for silver deposition process, and the substrate with the most charge transfer involved. Regarding the surface roughness and the charge transfer measured from cyclic voltammetry, we expected that larger number of active sites and faster 3D silver deposition growth will be seen at the FVC electrode and that HOPG will be the most inactive electrode. Interestingly, on analyzing other data from Table 2, no set of kinetic parameters had shown the expected trend of the RMS[Rq] series. The density of the formed silver nuclei Ns was found to be the highest for FVC and actually decreases in order from HOPG to MPVC. Using Ns as the criteria of deposit efficiency, one could say that most silver nuclei were formed at the FVC electrode, despite the fact that electrode substrate does not possess a higher number of active sites. In this context, it is also interesting to check the *N*s/N_0 ratio as a measure of the active sites use. The highest *N*s/N_0 ratio has MPVC substrate, and the lowest HOPG. In the case of the MPVC substrate, it is worthwhile to note that MPVC possesses the smallest number of active sites, but the efficiency of their use is much better than that on the HOPG substrate. An additional interesting thing is to check how much charge is associated with the formation of single silver nuclei at the electrode surface. To obtain this particular number, the value of *Q* needed to be divided by *N*s. With the exception of the transient with very low or very high overpotentials, the calculated values for charge-transfer associated with a single silver nuclei were FVC (from 3.61×10^{-6} mC to 8.44×10^{-6} mC), MPVC (from 1.21×10^{-5} to 2.49×10^{-5} mC), and HOPG (from 1.24×10^{-5} to 1.59×10^{-5} mC). Obviously, the smallest charge transfer is associated with the formation of silver nuclei on the FVC substrate. HOPG and MPVC show similar but higher charge consumption per silver nuclei, a possible explanation of such a difference in the charge consumption during the

silver nuclei formation can be related to the difference among silver nuclei characteristics or the nature of active sites on different substrates. Although the work on the identification of active sites and silver nuclei on different carbon electrode is in progress, we currently have no evidence to support one or another hypothesis.

The silver nucleation rate A, was also found to be different for different substrates. The highest A value was achieved during deposition onto the MPVC substrate and the slowest values into the HOPG substrates; interestingly, it is completely opposite to the trend observed for D (diffusion coefficient) values.

Just to make it clearer before discussing other issues, we would like to emphasize a major finding of this part of our study. Silver deposition onto HOPG, FVC, and MPVC substrates proceeds as a 3D diffusion-controlled nucleation and growth process. The HOPG substrate possesses the highest number of active sites for the deposition process, which generates the highest charge transfer and possibly the highest amount of deposit. However, the MPVC possesses the smallest number of formed silver nuclei (efficiency of the active sites use) as well as a very fast nucleation rate, much faster than that of the HOPG surface. Trends among kinetic data of the silver deposition do not correlate to those seen for the electrode surface roughness (RMS[Rq]) or the values of charge transfer measured from cyclic voltammetry. Note that FVC, with the highest surface roughness, was expected to be a substrate with the most active sites, the larger number of the formed nuclei, and the highest amount of deposit. Our results clearly showed a lack of direct correlation between the number of active sites for silver 3D deposition and the electrode surface morphology characteristics. It seems that, for silver 3D nucleation, the electrode surface morphology is of less importance than, for example, the number of active sites (N_0) or number of silver nuclei (Ns). The amount of charge associated with formation of single silver nuclei was found to be substrate dependent. A very low amount of charge was observed for silver nuclei on the FVC substrate, and the highest amount was observed for the MPVC electrode. We assume that it indicates additional processes (oxide) or the difference in the nature of active sites among different substrates.

In the final part, we wanted to show our efforts and discussion related to the correlation between the kinetic parameters of the silver 3D deposition (Table 2) and the surface morphology characteristics revealed by AFM imaging. In short, our intention was to use high-resolution AFM images for identification and characterization of substrate surface features as "potential" active sites for the silver deposition. It equally involves the visualization of a single active site as well as that of a larger surface area, to see if the number of the observed features corresponds to the N_0 values from chronoamperometric study. Although we did not succeed completely in our goal, the results obtained are worth being presented and discussed. During the study, many AFM images of different size were obtained; however, here, we refer our discussion to the images of Figure 1(a−c), due to practical reasons.

First of all, we would like to show the relationship between image size, density of the observed surface features in the image, and density of active sites for the silver deposition process from Table 2. All images in Figure 1 have the same size: 2 200 nm $\times$ 2 200 nm, which means that each image is showing a surface area of 4.84×10^6 nm^2. AFM images are presented in so-called "height" mode, with image features presented as three-dimensional objects with bright colors assigned to higher places. Because every substrate has a different morphology, we first classified surface features by shape and size. For example, in the case of HOPG, four large terraces with steps have been found. The surface of MPVC has a form of nodular features, ca. 250 nodules, each about 1.6×10^4 nm^2 of surface area. FVC also possesses a nodular texture but with larger number of features (ca. 500) of a smaller size (ca. 8.0×10^3 nm^2 per feature).

Led by the assumption that each surface feature seen in an AFM image eventually could become the "potential" active site for silver deposition, as a next step, we calculated the density of surface features and compared it with the number of deposition active sites N_0 (Table. 2.). The AFM images revealed that MPVC and FVC possess 5.16×10^9 features/cm^2 and 1.03×10^{10} features/cm^2, respectively. Again, following the assumption that each surface feature will provide at least one active site for deposition, one could expect that the number of active sites would correspond to the number of surface features. However, our results did not support such a simple picture. Note that in Table 2, the N_0 values vary from 0.50×10^6 to 1.53×10^6 active site/cm^2 for MPVC and from 1.40×10^6 active site/cm^2 to 14.07×10^6 active site/cm^2 for FVC, which, in comparison with AFM images, leads to the conclusion that there are more surface features than active sites or that not every surface feature seen in the AFM image will become the deposition active site. Indeed, it could be calculated that only one of the 3372 to 10 320 features on the MPVC surface, and only one of the 732 to 7357 features on the FVC substrate, will become the active sites for the silver deposition process. Although it seems to be a very simple analysis, these results indicate several quite important things concerning the metal electrocrystallization processes. First, and most intriguing, is a question of the active sites nature. We believe that because of such a big difference between the number of the observed surface feature and the number of active sites calculated from 3D deposition kinetics, it could be concluded that the nature of the active site is rather electronic and should be not defined as a physical feature on the electrode surface. That will also somehow explain why an increase in the surface roughness does not lead to a straight increase in the electrode activity, as well as the fact that silver 3D deposition process did not show real dependence toward changes in the electrode roughness. Obviously, the increase in the surface roughness means an increase in the number of surface features, but not necessarily in the number of the silver deposition active sites. In this sense, it will be very interesting to see how this correlates to the electrode activity, that is, the activation of active sites without an increase in the surface roughness and surface features on the electrode surface.

Because active sites are of rather unknown nature, their identification on the electrode surface is very questionable. Note that Scharifker and Mostany's theoretical models[44] are based on the hypothesis that considers the active sites as physical places on the originally "frozen" energetic state of the electrode surface. After applying the overpotential, the number of active sites on the electrode surface is instantaneously fixed. At the same time, Milchev[48−50] based his model of nucleation kinetics on the assumption that active sites may appear on and disappear from the electrode surface due to some independent electrochemical reactions, parallel to the nucleus formation (i.e., oxidation−reduction, surface transformation phenomena within preformed under potential deposition (UPD) layers, adsorption and desorption of anions, molecules, or impurities). Certainly, in terms of the possible visualization of active sites, we choose associate with the steady-state model. However, it still questions our approach because it is not sure that before applying potential

at the electrode, the "potential" or real active sites can be recognized at the electrode surface. To avoid any doubts, we reported our analysis, but this time using a number of silver nuclei *N*s (Table 2), instead of N_0, as an object to be compared with number of the surface features in AFM images. Note that silver nuclei can be treated as a physical object and according to literature, can be recognized more easily, even with microscopic techniques with lower resolution than AFM technique. For example, Serruya et al.[51] claimed an excellent agreement between the saturation number densities of nuclei obtained from current-transient measurements and micrographs obtained with metallographic microscope, for lead deposition on the vitreous carbon electrodes. Another example of the excellent agreement between the saturation number of densities for nuclei derived from analysis of current transients and those obtained from the direct microscopic observations, is reported for silver electrocrystallization from aqueous leaching solution onto vitreous carbon electrode.[52]

However, because *N*s is even smaller number than N_0, (lower density of silver nuclei than of active sites), the results of this new analysis still lead to the same conclusion that the number of silver nuclei is much smaller than the number of surface features imaged on the electrode surface. At this point, we also realized the fact that evaluation of the active sites or silver nuclei density, based on AFM imaging, will be a very difficult task. Namely, taking into account that the density of active sites and the density of silver nuclei is very low (see Table 2), it can be easily demonstrated that on imaging a small area, like one in Figure 1, one has very slim statistic chances to get even a single active site or nuclei in the particular image area. It is based on the assumption that we know how to recognize/distinguish such sites among from other surface features. To have at least one active site or silver nuclei in the image, statistically, one should increase the imaged area at least 30 to 200 times more than the images presented in Figure 1. It depends on N_0 and *N*s values and varies by substrate. Because active sites and nuclei are expected to be atomic size features, it is clear that such large areas, necessary to be imaged for statistical requirement, cannot be at the same time viewed with atomic resolution. In some cases, when the number of nuclei does not change during the deposition time (i.e., instantaneous nucleation with the same nuclei saturation density as the number of nuclei at the beginning of nucleation process), *N*s can be evaluated even by low resolution optical microscope.[51,52] Penner et al.[53] compared the number of silver nuclei (*N*s) on the HOPG electrode, obtained from current-transient analysis and AFM visualization. The experimental conditions were adjusted in such way that the very early stages of the instantaneous nucleation were monitored (large overpotentials: 100, 250, and 500 mV and short potential pulse in msec range). Excellent agreement between *N*s values from AFM analysis ($0.3-1.2 \times 10^{10}$ cm^{-2}) and electrochemical data were found only for larger overpotentials: 2.6×10^{10} cm^{-2} for 500 mV and 4.2×10^{9} cm^{-2} for 250 mV. For the 100 mV overpotential, *N*s lower for order of magnitude was determinate. For several valuable reasons, the *N*s values obtained in our study could not be compared with the previous results. In our study, silver deposition was performed under a different energetic regime, with significantly larger potential pulses and much smaller overpotential values (a progressive type of nucleation).

Another interesting example is work of Phillips and coworkers,[32] which followed slow changes in the electrode morphology during the deposition of thallium oxide onto glassy carbon electrode, using AFM. They found that the number, shape, and size of the deposited clusters change drastically during the progress of deposition. In fact, the electrode crystalline changed during the different phases of growth, which challenges the optical microscope approach because it is clear that in order to be seen with a low resolution optical microscope, the deposit must be in the very late stage of growth (large) and could have completely different characteristics than the nuclei initially formed on the electrode surface.

4. Conclusions

This study is dealing with a silver electrocrystallization process onto a carbon electrode substrate, as the earliest stage of the silver bulk deposition. The deposition was carried out from 10^{-2} M $Ag(NH_3)_2^+$/1.6 M NH_3, 1 M KNO_3 (pH = 11) electrolyte solution, on three rather typical carbon electrodes: HOPG, MPVC, and FVC. As verified by AFM imaging, just before the silver deposition process, each of the electrodes used possesses its own characteristic surface morphology. Indeed, the AFM images revealed details of the surface structure, shape, and size of typical surface features and surface roughness (via RMS[Rq} factor), which were the base for qualitative and quantitative evaluation of the electrode surface morphology.

The main aim of our study was to determine a possible influence and establish a relation between the carbon electrode surface morphology and the course of the silver electrocrystallization process. It is a topic of special interest because electrocrystallization process exclusively proceeds via deposition active centers and deposit nuclei formation mechanism, which could not necessarily be the function of macroscopic characteristic of the electrode surface.

The electrochemical techniques, cyclic voltammetry and chronamperometry, have been used to study the silver electrocrystallization process. Cyclic voltammetry offers a more general type of parameters helpful to characterize the position (potential) of the silver deposition\dissolution peaks, total charge related to deposition, and silver dissolution process. Interestingly, the silver deposition\dissolution peaks were always found on the same potentials regardless the carbon substrate used. However, the total amount of charge related to silver deposition or dissolution process was found to have a direct relationship to the electrode surface roughness (RMS[Rq] factor). The trend among the obtained data is very clear, more charge, which could also be extrapolated to more silver deposition, is associated with the carbon surface with higher surface roughness. Thus, the silver deposition efficiency was found to be the highest on FVC electrode (the highest surface roughness), and decreases for MPVC to HOPG (the lowest efficiency and the lowest surface roughness). The simplest explanation seems to be a relation between the silver deposition efficiency and the electrode active area (increase due to the surface roughness). However, as our analysis shows, the relation is not straightforward (linear), and an increase in the electrode surface roughness is not proportionally followed by an increase in the deposition charge (silver deposit), which clearly indicates that apart from surface morphology other factors must have influence on the electrocrystallization process, too.

To obtain more specific information about the silver electrocrystallization process, in particular, as for the characteristics related to the electrode surface conditions and the mechanism of surface processes, a chronoamperometric study was performed. The research was based on the current-transient measurements, their analysis and evaluation of characteristic kinetic parameters for silver electrocrystallization (nucleation and growth) process. Detailed analysis of the recorded current transients and their comparisons with adequate theoretical

models clearly indicate that on all three carbon substrates, silver deposition can be classified as a 3D electrocrystallization process controlled by silver ions diffusion kinetic. However, the process takes place in different potential ranges in dependence on the substrate used (or the substrate surface characteristics). The amount of overpotential necessary to initiate a 3D silver deposition reaction raises from HOPG, over FVC to MPVC electrode surface. We suppose that the observed trends are related to electrode surface conditions, including surface morphology and the fact that MPVC electrode is most probably covered with some kind of oxide adlayer, as a result of polishing procedure.

On all three surfaces, at lower overpotentials, the current transients are closer to the progressive type, but the increase in overpotential leads to a shift to instantaneous type. Further analysis of kinetic parameters of the silver deposition process involved estimation of nucleation rate (A), number density of active sites (N_0), saturation number density of the formed silver nuclei (Ns) and charge during the first 20 s of potentiostatic transients of the silver electrocrystallization process (Q). Although there are parameters that define kinetics of silver deposition process, their sensitivity to electrode surface conditions make them useful in the evaluation of the electrode surface quality. Apart from some expected and rather regular behavior of such A, N_0, Ns, and Q at with overpotential, found for all three substrates, we also found that HOPG possesses higher numbers of N_0 and charge density Q. The minimum N_0 was recorded on the MPVC electrode. However, the density of formed silver nuclei was found to be the highest on the FVC substrate, and gradually drops to a lower value on HOPG and MPVC, respectively. The Ns/N_0 ratio (efficiency of active sites use) was found to be the highest on MPVC substrate. Thus, HOPG possesses the highest active sites number, but does not use all of them so efficiently as they are employed on MPVC substrate. The charge consumed per a formed silver nuclei also appears as a very interesting parameter. The smallest charge transfer was found to be associated with formation of silver nuclei on the FVC electrode substrate. As a final aim, we attempted to relate the difference among kinetic parameters obtained on different substrates to the quality and conditions on the carbon electrode surface (i.e., surface roughness factor). Our results clearly show a lack of a straight and simple relation, which could connect two such sets of parameters. The electrocrystallization process seems to be a very specific reaction that proceeds over a very small portion of the electrode surface, in and around the active sites zones, which possibly have very specific characteristics in the sense of the surface structure and electronic properties. Therefore, macroscopic parameters like, surface roughness, number of surface features, and surface morphology characteristics, visualized by AFM images, do not really have relationships with such surface limited processes. As discussed in the last part of paper, further progress and better understanding of a metal electrocrystallization process on foreign substrates is limited by the poor understanding of the active site meaning and low possibility for their visualization by the microscopic techniques.

Acknowledgment. This work was financially supported by CONACyT (Project 0913E-P, Project L0081-E9608 and Cátedra Patrimonial de Excelencia Nivel II-32158E.). M. Miranda-Hernández, acknowledge CONACyT for Ph.D. scholarship.

References and Notes

(1) van der Linden, E. W.; Dieker, J. W. *Anal. Chim. Acta* **1980**, *119*, 1.
(2) Kelpy, L. J.; Bard, A. J. *Anal. Chem.* **1988**, *60*, 1459.
(3) McCreery, R. L. Carbon Electrodes: Structural Effects on Electron-Transfer Kinetics. In *Electroanalytical Chemistry. A Series of Advances*; Bard, A.J., Ed.; Marcel Dekker: New York, 1991 Vol. 17, p 221.
(4) Rusling, J. F. *Anal. Chem.* **1984**, *56*, 575.
(5) Poon, M.; McCreery, R. L. *Anal.Chem.* **1986**, *58*, 2745.
(6) Wightman, R. M.; Deakin, M. R.; Kovach, P. M.; Kuhr, W. G.; Stutts, K. J. *J. Electrochem. Soc.* **1984**, *131*, 1578.
(7) Hu, I. F.; Karweik, D. H.; Kuwana, T. *J. Electroanal. Chem.* **1985**, *188*, 59.
(8) Rice, R.; Allred, C.; McCreery, R. *J. Electroanal. Chem.* **1989**, *263*, 163.
(9) Rice, R. J.; Pontikos, M. N.; McCreery, R. L. *J. Am. Chem. Soc.* **1990**, *112*, 4617.
(10) McDermott, M. T.; Kneten, K.; McCreeery, R. L. *J. Phys. Chem.* **1992**, *96*, 3124.
(11) Chen, Q.; Awain, G. M. *Langmuir* **1998**, *14*, 7017.
(12) Kamau, G. N.; Willis, W. S.; Rusling, J. F. *Anal. Chem.* **1985**, *57*, 545.
(13) Bodalbhai, L.; Brajter-Toth, A. *Anal. Chem.* **1988**, *60*, 2557.
(14) Hance, G. W.; Kuwana, T. *Anal. Chem.* **1987**, *59*, 131.
(15) Evans, J. F.; Kuwana, T. *Anal. Chem.* **1977**, *49*, 1632.
(16) Engstrom, R. C.; Strasser, V. A. *Anal. Chem.* **1984**, *56*, 136.
(17) Kazee, B.; Weisshaar, D. E.; Kuwana, T. *Anal. Chem.* **1985**, *57*, 2739.
(18) Enstrom, R. C.; Johnson, D. W.; DesJarlais, S. *Anal. Chem.* **1987**, *59*, 670.
(19) Gewirth, A. A.; Bard, A. J. *J. Phys. Chem.* **1988**, *92*, 5563.
(20) Lee, C.W.; Bard. A. J. *J. Electroanal. Chem.* **1988**, *135*, 1599.
(21) Wang, J.; Martinez, T.; Yaniv, D. R.; McCormick, L.D. *J. Electroanal. Chem.* **1990**, *278*, 379.
(22) Bodalbhai, L.; Brajter-Toth, A. *Anal. Chim. Acta* **1990**, *231*, 191.
(23) Pontikos, M. N.; McCreery, R. L. *J. Electroanal. Chem.* **1992**, *324*, 229.
(24) McDermott, M. T.; McDermott, C. A.; McCreery, R. L. *Anal. Chem.* **1993**, *65*, 937.
(25) Budevski, E.; Staikov, G.; Lorenz, W. J. *Electrochemical Phase Formation and Growth*; VCH: New York, Chapter 1, 1996.
(26) Carreño, G.; Sosa, E.; Gonzalez, I.; Ponce-de-Leon, C.; Batina, N.; Oropeza, M. T. *Electrochim. Acta* **1999**, *44*, 2633.
(27) Sosa, E.; Carreño, G.; Ponce-de-León, C.; Oropeza, M. T.; Morales, M.; González, I.; Batina, N. *Appl. Surf. Sci.* **2000**, *153*, 245.
(28) Miranda-Hernández, M.; Palomar-Pardavé, M.; Batina, N.; González, I. *J Electroanal. Chem.* **1998**, *443*, 81.
(29) Palomar-Pardavé, M.; Miranda-Hernández, M.; González, I.; Batina, N. *Surf. Sci.* **1998**, *399*, 80.
(30) Palomar-Pardavé, M.; Ramírez, M. T.; González, I.; Serruya, A.; Scharifker, B. R. *J. Electrochem. Soc.* **1996**, *143*, 1551.
(31) Jowal, K.; Xie, L.; Hug, R.; Farrington, G. C. *J. Electrochem. Soc.* **1992**, *139*, 2818.
(32) Phillips, R. J.; Golden, T. D.; Shumsky, M. D.; Switzer, J. A. *J. Electrochem. Soc.* **1994**, *141*, 2391.
(33) Aubach, D.; Cohen, Y. *J. Electrochem. Soc.* **1996**, *143*, 3525.
(34) Li, Y. G.; Lasia, A. *J. Appl. Electrochem.* **1997**, *27*, 643.
(35) Bard, A. J.; Faulkner, L. J. In *Electrochemical Methods-Fundamental and Application*; John Wiley & Sons: New York, 1980.
(36) Freund, M. S.; Brajter-Toth, A.; Cotton, T. M.; Henderson, E. R. *Anal. Chem.* **1991**, *63*, 1047.
(37) Li, J.; Wang, E. *Electroanalysis* **1996**, *8*, 107.
(38) Anderson, J. L.; Bowden, E. F.; Pikcup, P. G. *Anal. Chem.* **1996**, *68*, 379R.
(39) Lorenz, W. J.; Schmidt, E.; Staikov, G.; Bort, H. *Faraday Symp. Chem. Soc.* **1977**, *12*, 14.
(40) Scharifker, B. R.; Hills, G. *Electrochim. Acta* **1983**, *28*, 879.
(41) Pauling, H. J.; Jüttner, K. *Electrochim. Acta* **1992**, *37*, 2237.
(42) Fletcher, S.; Halliday, C. S.; Gates, D.; Westcott, M.; Lwin, T.; Nelson, G. *J. Electroanal. Chem.* **1983**, *159*, 267.
(43) Czerwiski, A.; Helszowska, M. *J. Electroanal. Chem.* **1996**, *410*, 55.
(44) Scharifker, B.R.; Mostany, J. *J. Electroanal. Chem.* **1984**, *177*, 13.
(45) Mostany, J.; Mozota, J.; Scharifker, B. R. *J. Electroanal. Chem.* **1984**, *177*, 25.
(46) Mostany, J.; Parra, J.; Scharifker, B. R. *J. Appl. Electrochem.* **1986**, *16*, 333.
(47) Tsakova, V.; Milchev, A. *J. Electroanal. Chem.* **1987**, *235*, 237.
(48) Milchev, A. *Electrochim. Acta* **1985**, *30*, 125.
(49) Milchev, A. *Electrochim. Acta* **1986**, *31*, 977.
(50) Milchev, A *J. Electroanal. Chem.* **1998**, *457*, 35.
(51) Serruya, A.; Mostany, J.; Scharifker, B. R. *J. Chem. Soc. Faraday Trans.* **1993**, *89*, 255.
(52) Serruya, A.; Scharifker, B. R.; González, I.; Oropeza, M. T.; Palomar-Pardave, M. *J. Appl. Electrochem.* **1996**, *26*, 451.
(53) Zoval, J. V.; Stiger, R. M.; Biernacki, P. R.; Penner, R. M. *J. Phys. Chem.* **1996**, *100*, 837.